doi:10.1006/jmbi.2001.4449 available online at http://www.idealibrary.com on IDEAL® *J. Mol. Biol.* (2001) **307**, 309–322

JMB

Self-association Reaction of Denatured Staphylococcal Nuclease Fragments Characterized by Heteronuclear NMR

Keqiong Ye and Jinfeng Wang*

National Laboratory of Biomacromolecules, Institute of Biophysics, Chinese Academy of Sciences, 15 Datun Road Beijing 100101, China

*Corresponding author

The self-association reaction of denatured staphylococcal nuclease fragments, urea-denatured G88W110, containing residues 1-110 and mutation G88W, and physiologically denatured 131-residue Δ131Δ, have been characterized by NMR at close to neutral pH. The two fragments differ in the extent and degree of association due to the different sequence and experimental conditions. Residues 13-39, which show significant exchange line broadening, constitute the main association interface in both fragments. A second weak association region was identified involving residues 79-105 only in the case of urea-denatured G88W110. For residues involved in the association reaction, significant suppression of the line broadening and small but systematic chemical shift variation of the amide protons were observed as the protein concentration decreased. The direction of chemical shift change suggests that the associated state adopts mainly β-sheet-like conformation, and the β-hairpin formed by strands β2 and β3 is native-like. The apparent molecular size obtained by diffusion coefficient measurements shows a weak degree of association for Δ131Δ below 0.4 mM protein concentration and for G88W110 in 4 M urea. In both cases the fragments are predominantly in the monomeric state. However, the weak association reaction can significantly influence the transverse relaxation of residues involved in the association reaction. The degree of association abruptly increases for Δ131Δ above 0.4 mM concentration, and it is estimated to form a 4 to 8 mer at 2 mM. It is proposed that the main region involved in association forms the core structure, with the remainder of residues largely disordered in the associated state. Despite the obvious influence of the association reaction on the slow motion of the backbone, the restricted mobility on the nanosecond timescale around the region of strand β5 is essentially unaffected by the association reaction and degree of denaturation.

Keywords: staphylococcal nuclease; protein self-association; backbone dynamics; residual structure; denatured protein

Introduction

Proteins may self-associate both *in vivo* and *in vitro*.[1] More than a dozen proteins assemble *in vivo* into amyloid fibrils which are related to diseases, such as Alzheimer's disease and Parkinson's disease.[2] Recombinant proteins frequently form inclusion bodies in *Escherichia coli*.[3] In protein folding studies, denatured proteins are prone to form aggregates,[4–8] which may be mistaken for folding intermediates.[9] Despite the importance of protein aggregation, its mechanism is still not well understood.

Abbreviations used: SNase, staphylococcal nuclease; Δ131Δ, SNase fragment with residues 1-3 and 13-140; G88W110, SNase fragment with residues 1-110 and mutation G88W; NMR, nuclear magnetic resonance; R_1, longitudinal relaxation rate; R_2, transverse relaxation rate; R_{2ex}, exchange contribution to R_2 rate; R_{2asso}, exchange contribution to R_2 rate due to the association reaction; CPMG, Carr-Purcell-Meiboom-Gill; HSQC, heteronuclear single-quantum coherence; NOE, nuclear Overhauser effect.

E-mail address of the corresponding author: jfw@sun5.ibp.ac.cn

0022-2836/01/010309–14 $35.00/0

Staphylococcal nuclease (SNase) with 149 residues has long been used as a model system in protein folding studies. The structure of SNase (Figure 1) consists of five β-strands and three α-helices.[10] The β-strands and helix α1 form an ''OB-fold'',[11] the architecture of which is shared by a number of other non-homologous proteins, for example, the cold shock protein A (CspA)[12] and the anticodon binding domain of lysyl-tRNA synthetase (LysN).[13] The three OB-fold proteins, SNase, CspA and LysN, have recently been shown to self-associate in acidic conditions.[5–8]

Here, we report that denatured SNase can self-associate to form soluble aggregates at close to neutral pH. Two denatured fragments Δ131Δ and G88W110 have been characterized by NMR spectroscopy. Fragment Δ131Δ, consisting of residues 1-3 and 13-140, is denatured under physiological conditions, and it has been extensively analyzed as a denatured model in the absence of denaturants.[12–20] It has been shown that the resonances from residues 13-39 are broadened out beyond the detectable limit in the NMR spectra of Δ131Δ due to intermediate chemical exchange (millisecond to microsecond). A monomeric state has been assumed in previous investigations of Δ131Δ.[12–20] Fragment G88W110, consisting of residues 1-110 with mutation G88W, can fold into a stable and native-like structure under physiological conditions, corresponding to the part of the native structure that contains the OB-fold[21] (K.Y. & J.W., unpublished results). The urea-denatured states of G88W110 are studied here.

The region involved in association and the multimerization degree of the two denatured fragments have been probed by following the concentration dependence of the line broadening, the H_N chemical shifts and the apparent molecular size. We conclude that the chemical exchange observed for residues 13-39 of denatured SNase mainly result from the association reaction, not from the intramolecular motion. The previously reported restricted backbone dynamics on the nanosecond timescale around strand β5 of denatured Δ131Δ,[13] however, is observed here to be essentially unaffected by the association reaction and the degree of denaturation.

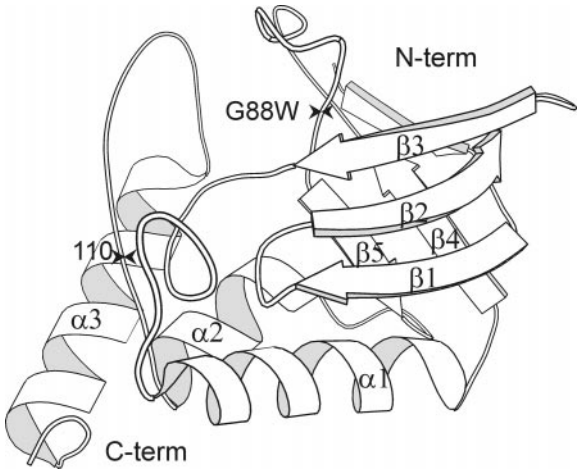

Figure 1. Molscript[45] representation of native staphylococcal nuclease.[10] The three helices (α1, 54-68; α2, 98-106; α3, 121-135), five β-strands (β1, 13-19; β2, 21-27; β3, 29-35; β4, 71-75; β5, 91-95) are labeled. Five β-strands and helix α1 form an OB-fold. The mutation and truncation sites in the G88W110 fragment are marked.

Results

NMR assignments

Characterization of the association reaction at the residue level was made possible by complete resonance assignments for ^{13}C and ^{15}N double-labeled G88W110 in 6 M urea. Assignment strategies for the denatured proteins have been described.[22] Three pairs of experiments, CBCA(CO)NH/HNCACB, HNCO/HN(CA)CO and H(CCO)NH/15N-TOCSY, established the connectivity of the neighboring residues *via* backbone resonances as well as side-chain protons. The plentiful correlations they provided allowed unambiguous assignment of the degenerate resonances. All 104 non-proline and non-N-terminal residues in G88W110 can be assigned in the ^{1}H-^{15}N HSQC spectrum measured in 6 M urea (Figure 2). Overlapped residues include L25/K45/A102, F34/K53, R35/I72, L36/K63, L37/R105, Y54/R87 and K78/W88. The spectrum measured in 4 M urea is similar to the spectrum in 6 M urea, except that the residues K5/L7, L14/A109, E43/N68, R81/D83 and N100/E101 are overlapped and residues Y54/R87 become separated. The complete assignment of denatured G88W110 in 6 M urea is provided as supplementary material and has been deposited in the BioMagResBank (http://www.bmrb.wisc.edu) under BMRB accession number 4905.

The chemical shifts of denatured G88W110 are similar to those of Δ131Δ[12,17] and Δ131Δ in 6 M urea.[15] However, several residues in G88W110 in 6 M urea show significant upfield shifted backbone and side-chain proton resonances compared with the same type of amino acid at other positions in the polypeptide chain, which was not reported previously for Δ131Δ.[12,17] These residues include K84 ($H^{\alpha} = 4.11$; $H^{\beta} = 1.58$; $H^{\gamma} = 1.07$, 0.99; $H^{\varepsilon} = 2.85$), L89 ($H_N = 8.04$; $H^{\alpha} = 4.23$; $H^{\beta} = 1.47$; $H^{\gamma} = 1.40$; $H^{\delta} = 0.81$), A90 ($H_N = 8.02$; $H^{\alpha} = 4.15$; $H^{\beta} = 1.27$) and I92 ($H_N = 7.88$; $H^{\alpha} = 4.09$; $H^{\beta} = 1.66$; $H^{\gamma 2} = 0.71$; $H^{\gamma 1} = 1.23$, 0.99). The upfield shifts may possibly be due to ring current effects from the abundance of aromatic residues (Y85, W88, Y91 and Y93) and the compact conformation in this region.[17]

Concentration-dependent line broadening

In moderate urea concentrations (2-4 M), amide resonances of residues located in the β2 and β3 region of G88W110 show clearly reduced intensi-

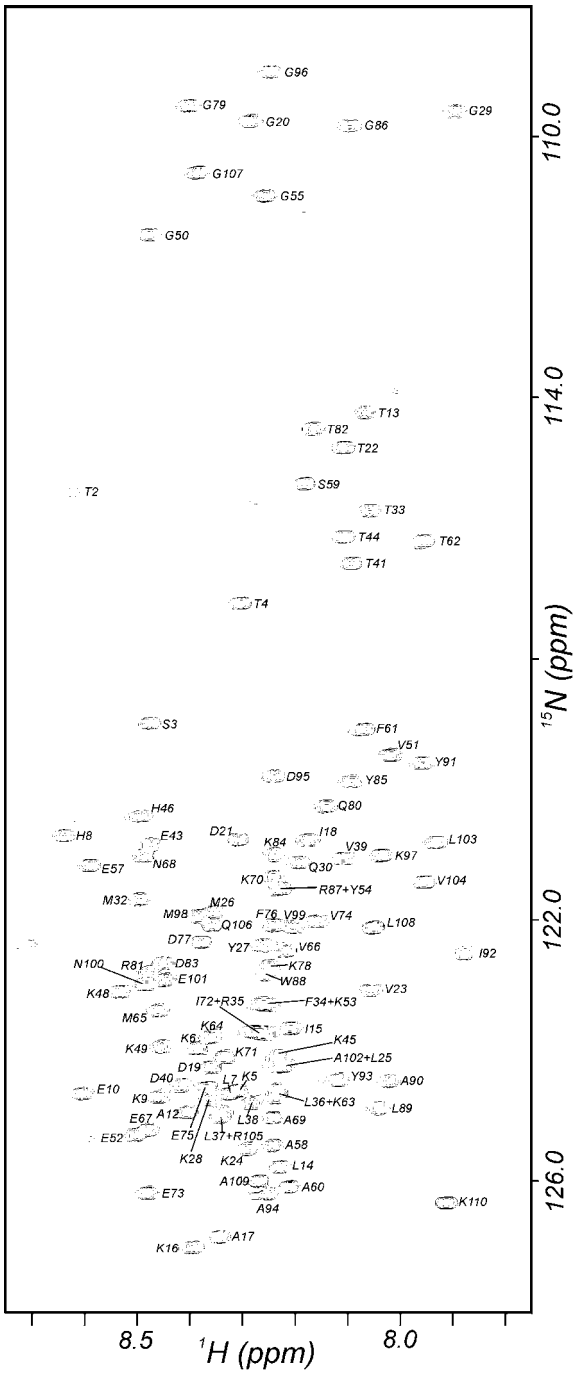

Figure 2. ^{1}H-^{15}N HSQC spectrum of the G88W110 fragment of staphylococcal nuclease in 6 M urea, pH 4.9 and 305 K. Sequence assignments are indicated for all 104 non-proline and non N-terminal residues.

ties in the HSQC spectra due to line broadening (data not shown). However, the line broadening is critically dependent on the protein concentration. Figure 3(a) shows the ^{15}N transverse relaxation rate R_2 of G88W110 in 4 M urea measured at protein concentrations of 1.5, 0.4 and 0.1 mM. At these conditions, most peaks are quantifiable and the concentration dependence of the line broadening is clear. Because of the excellent NMR relaxation properties, the R_2 rates could be accurately obtained for the unfolded polypeptide at protein concentrations as low as 0.1 mM. The mean R_2 rates (±s.d.) of all residues are 4.9(±2.7), 3.9(±1.6) and 3.6(±1.1) Hz for 1.5, 0.4 and 0.1 mM protein concentrations, respectively.

Intermediate exchange (milli- to microsecond) would increase the R_2 rate by an exchange component (R_{2ex}) and lead to line broadening of resonances. In principle, chemical exchange may result from intramolecular or intermolecular interactions, which can be distinguished by examining the dependence of line broadening on protein concentration. As indicated by the concentration dependence of the R_2 rate (Figure 3(a)), the chemical exchange process which increases the R_2 rate is not a single-molecular process, but must involve an intermolecular association reaction.

The change of the R_2 value between 1.5 mM and 0.1 mM protein concentrations is plotted in Figure 3(b) to show the R_{2ex} component arising from the association reaction (R_{2asso}). Residues 13-39 can be considered as the main association interface, since they have the largest R_{2asso} component. In addition, the association reaction weakly but significantly influences the R_2 rates of residues 79-105, which is referred to as the second association region.

In the absence of urea, the denatured Δ131Δ fragment under physiological conditions shows even more severe line broadening. Similar to the previous reports,[12,15] residues 13-44 are invisible in the ^{1}H-^{15}N HSQC spectrum of the 1.5 mM sample (Figure 4(a)). When the protein concentration is diluted to 0.1 mM, however, most of these resonances become detectable (Figure 4(b)). The residues with the most dramatic intensity changes are from strand β1 and the periphery of the main association region. It can be seen that residues T13 to T22 and residues D40 to T44 have normal intensity levels at 0.1 mM protein concentration. However, residues from strands β2 and β3 remain quite weak at 0.1 mM protein concentration and the intensities do not increase significantly at 20 μM protein concentration. Figure 4(c) shows the relative intensity of some identifiable residues around the main association region as a function of protein concentration. The general increase of the relative intensities of these residues indicates the reduction of the association degree when the protein concentration is decreased from 1.5 mM to 20 μM. The corresponding second association region observed in urea-denatured G88W110 was not observed for Δ131Δ.

Concentration-dependent amide proton chemical shift

A small but systematic change in the H_N chemical shifts in 4 M urea-denatured G88W110 was observed accompanying the relative intensity variation of resonances as the sample concentration

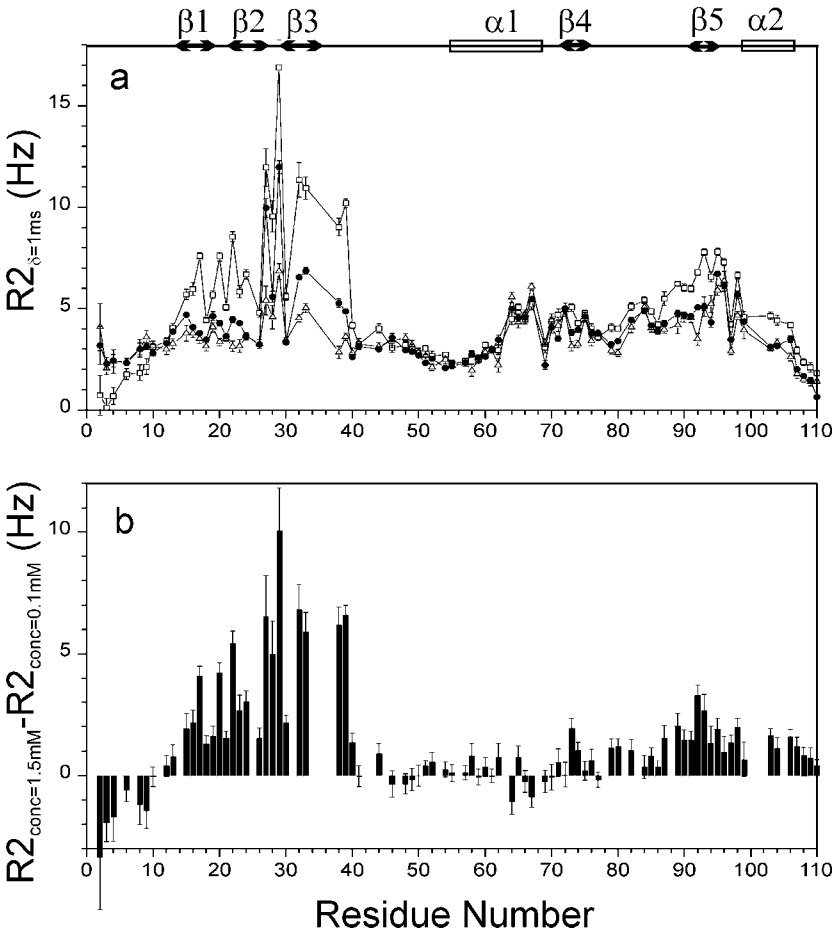

Figure 3. Transverse ^{15}N relaxation rates (R_2) for the G88W110 fragment in 4 M urea. (a) R_2 rates ($\delta = 1$ ms) were obtained at protein concentrations of 1.5 mM (open square), 0.4 mM (filled circle) and 0.1 mM (open triangle). (b) Difference of R_2 rates between 1.5 mM and 0.1 mM samples, manifesting R_2 increase (R_{2asso}) due to the association reaction. The secondary structures in the folded state are shown at the top of the Figure.

changed. Figure 5(a) shows the H_N chemical shift difference between 1.5 and 0.1 mM G88W110 in 4 M urea. The H_N chemical shift deviation between 0.4 mM and 0.1 mM samples is about 30 % of the total deviation between 1.5 mM and 0.1 mM samples. Residues 23-37 in the main association region show the most significant variations ranging from 0.01 to 0.02 ppm. The positive chemical shift variations, less than 0.01 ppm, were consistently observed to involve residues 76-103, which corresponds to the second association region. These variations are unlikely to be caused by errors in the chemical shift measurement, since residues outside the association region have a random pattern of variation.

Because the chemical shift is a population averaged property in the fast to intermediate NMR exchange timescale (demonstrated by a single set of peaks), the changes of chemical shift must arise from an increased population of associated species at the higher protein concentration. Based on the correlation between the secondary structure of the protein and the direction of deviation of chemical shifts,[23] the positive H_N chemical shift changes suggest that residues in the associated state adopt mainly β-sheet-like conformation. In particular, a native-like β-hairpin of strands β2 and β3 is most likely preserved in the associated state, since these residues in the associated state show a native-like pattern of chemical shift deviation when comparing with the H_N chemical shift deviation between the folded state and the unfolded state (Figure 5(b)). It is of note that residue Q30 has a unique negative deviation of H_N chemical shift in both the native state and the associated state.

The fraction of associated species can be estimated from the magnitude of the H_N chemical shift change which is proportional to the population variation of aggregate. The ratios of association-induced H_N chemical shift deviations to the secondary chemical shifts of the folded state, ranging from 1 to 5 %, are shown for residues 23-37 in the inset of Figure 5(a). The ^{15}N chemical shifts of residues 23-37 also change with similar magnitude (~2 %) in the direction of the native-like state. Assuming that there is 100 % of monomer in 0.1 mM G88W110 in 4 M urea as suggested by its rather uniform R_2 rates, the ratios of deviation suggests that approximately 1-5 % of molecules associate to form the native-like β-hairpin for 1.5 mM G88W110 in 4 M urea. The range can be regarded as a lower limit estimation of the population of associated species considering that the actual associated state is expected to be dynamic and less native like.

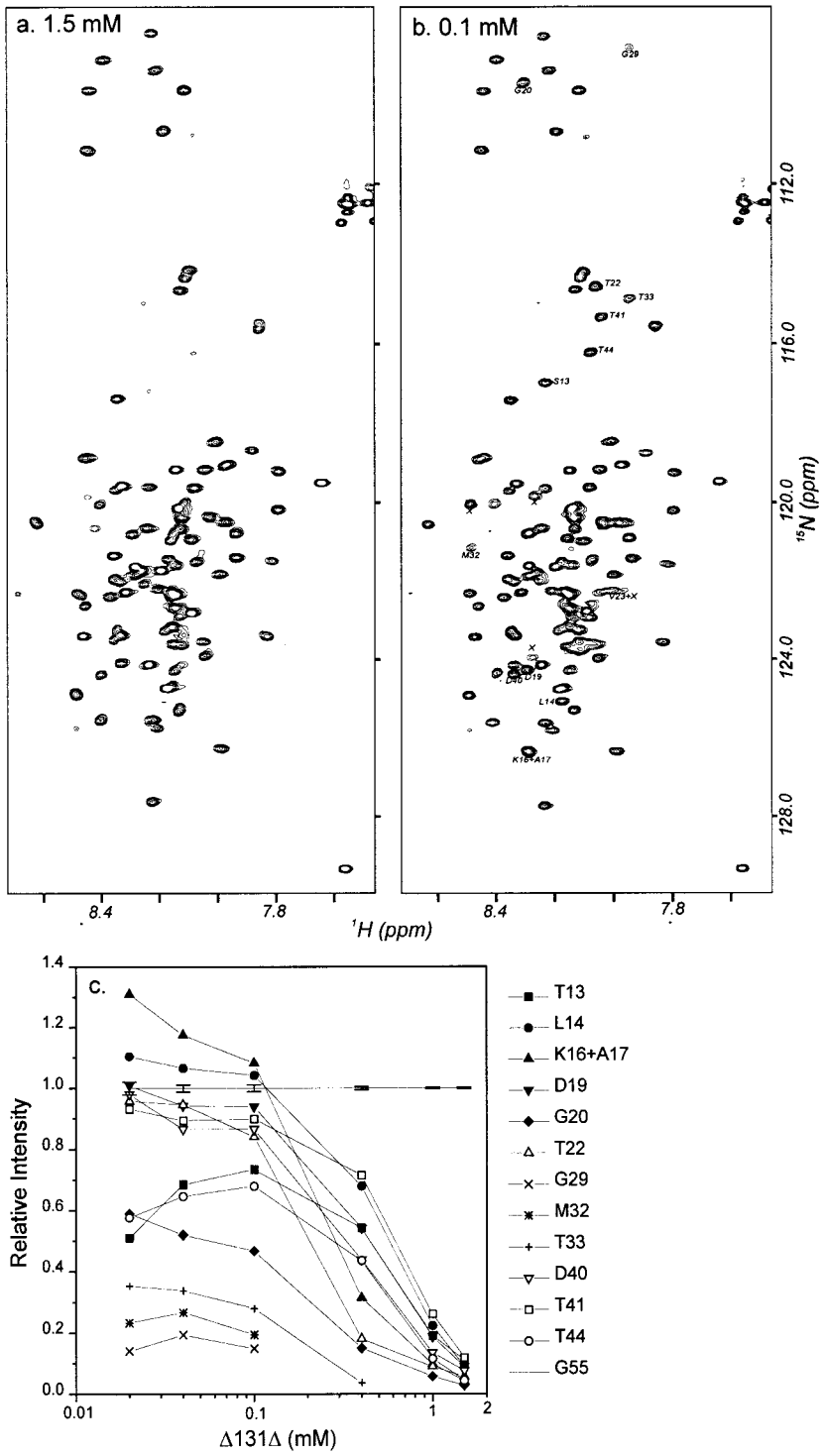

Figure 4. ^{1}H-^{15}N HSQC spectra of the Δ131Δ fragment of staphylococcal nuclease at pH 5.3 and 305 K with protein concentrations of (a) 1.5 mM and (b) 0.1 mM. Labeled peaks were tentatively assigned on the basis of the G88W110 assignments obtained in 6 M urea and with reference to previous assignments.[16] (c) Graphs of the relative amide intensity (normalized to the intensity of residue G55 which shows no exchange line broadening) in the ^{1}H-^{15}N HSQC spectra as a function of sample concentration. Residues from strands β2 and β3 are quite weak even at 20 μM protein concentration. The error bar in the G55 data point was calculated as the ratio of root-mean-square noise of the spectra to the G55 intensity.

Concentration-dependent molecular size

To assess the degree of aggregation, the apparent molecular size was obtained by diffusion coefficient measurements as a function of protein concentration. The results are shown in Figure 6. The diffusion coefficient D is inversely proportional to the effective hydrodynamic radius R according to the Stokes-Einstein equation:

$$D = kT/(6\pi\eta R) \quad (1)$$

where k is the Bolzmann constant, T is the temperature and η is the fluid viscosity.

The diffusion coefficient of the protein was measured by pulsed-field gradient NMR.[24,25] This method has been employed to study protein aggregation and protein unfolding.[26,27] In order to derive the protein radii, we calculated the diffusion coefficient ratio of the reference molecule dioxane to the

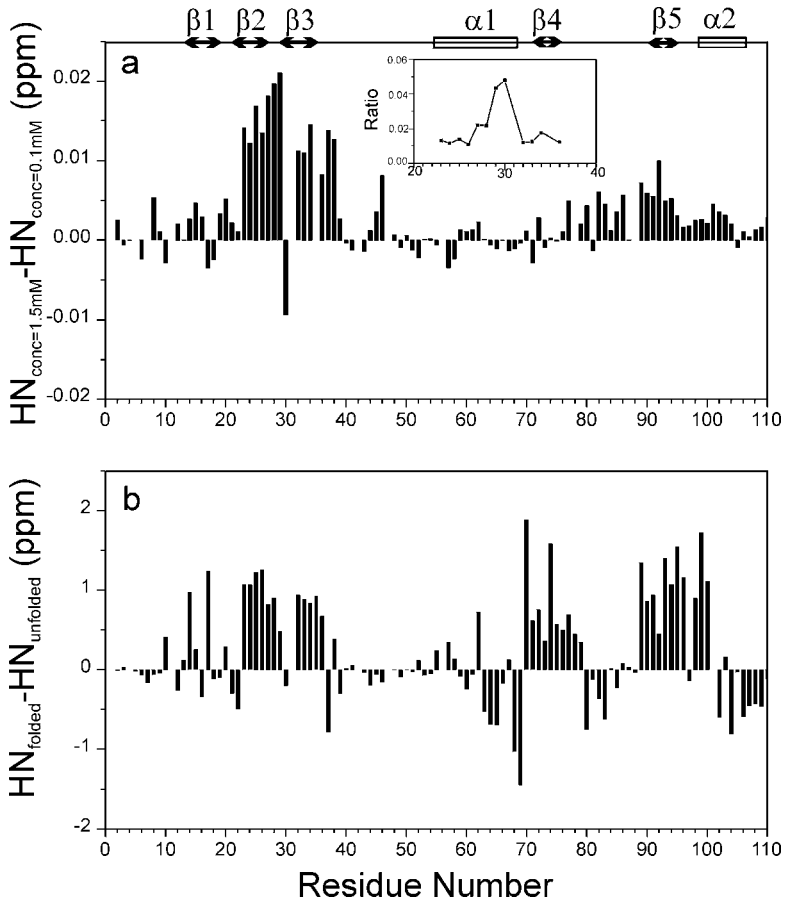

Figure 5. (a) Concentration-dependence of H_N chemical shift for G88W110 in 4 M urea. Shown is the H_N chemical shift of the 1.5 mM sample minus that of the 0.1 mM sample. The uncertainty of the H_N chemical shift was estimated to be less than 0.005 ppm. The positive change indicates the structure formed in the associated state is a β-sheet-like structure. (b) The H_N chemical shift difference between the folded (K.Y. & J.W., unpublished results) and unfolded state in 6 M urea of G88W110 fragment. The inset in (a) illustrates the ratio of the association-induced H_N chemical shift deviation (a) to the secondary chemical shift of the folded state (b) for residues 23-37 which exhibit the most significant H_N chemical shift deviation upon association.

protein ($D_{dioxane}/D_{protein}$), which is equal to the ratio of the apparent radius of the protein to that of dioxane. The ratio $D_{dioxane}/D_{protein}$ can then be converted to the apparent molecular radius R with reference to wild-type SNase which has a known radius of 16.2 Å[28] and a $D_{dioxane}/D_{protein}$ ratio of 10.7 measured under the same experimental conditions.

The calculation of the ratio $D_{dioxane}/D_{protein}$ also serves to account for possible viscosity changes in solutions with different protein and urea concentrations.[26] In fact, we have observed that the protein concentration has negligible effect on the solution viscosity, as indicated by the invariant $D_{dioxane}$ of $10.00(\pm 0.18) \times 10^{-10}$ m^2 s^{-1} at varying concentrations of Δ131Δ. Therefore, the mean $D_{dioxane}$ value was used to calculate the Δ131Δ ratios. Since only three conditions were measured for G88W110 in 4 M urea and the statistical estimation cannot be obtained, the individually measured $D_{dioxane}$ values were used to calculate the G88W110 ratios. The indicated errors in the $D_{dioxane}/D_{protein}$ ratios are due to the errors in both the $D_{dioxane}$ and the $D_{protein}$ values.

The apparent molecular radius of Δ131Δ increases abruptly when the protein concentration is increased above 0.4 mM (Figure 6), indicating the formation of multimers. The radius decreases about 10% as the concentration of Δ131Δ is decreased from 0.4 mM to 10 μM. For G88W110 in 4 M urea, the apparent molecular radius decreases approximately 14% as the protein concentration changes from 1.5 mM to 0.1 mM. The molecules at concentrations below 0.4 mM for Δ131Δ and below 1.5 mM for G88W110 are comparable in size with another denatured SNase fragment 1-136 which has a radius of 21.2 Å in the monomeric state,[28] suggesting that a large fraction of denatured protein is in a monomeric state under these conditions.

Backbone dynamics of G88W110 in 6 M urea

It has been shown that the association reaction can significantly influence the slow motions (milli- to microsecond) of residues involved in association. To investigate the influence of the association reaction and the degree of denaturation on the backbone dynamics in the high frequency region (nano- to picosecond), we characterized the backbone dynamics of G88W110 in 6 M urea, which can be compared with the dynamics of Δ131Δ at non-denaturing conditions.[13]

The ^{15}N longitudinal (R_1), transverse (R_2) relaxation rates and steady-state {^1H-^{15}N} NOE enhancements were measured at 14.1 T for G88W110 in 6 M urea at protein concentrations of 1.5 mM and 0.4 mM, under which conditions the degree of self-association is low. The relaxation data were then

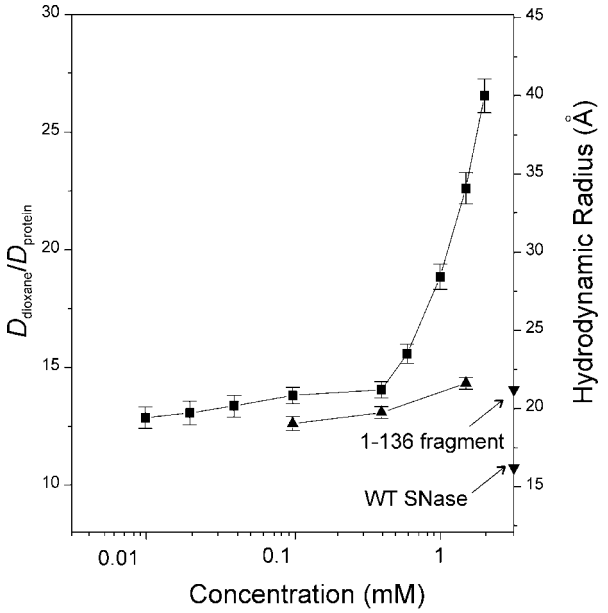

Figure 6. Diffusion coefficients for Δ131Δ without urea (filled square) and G88W110 in 4 M urea (filled triangle) as a function of protein concentration. All samples were in ^2H_2O with no buffer at 305 K. The monomeric radii of wild-type SNase and a SNase fragment containing residues 1-136 are shown.[28]

converted to the values of the spectral density function $J(\omega)$ at 0 MHz, 60 MHz (ω_N), and approximately 540 MHz ($\omega_H + \omega_N$) using reduced spectral density mapping. Reduced spectral density mapping has been shown to be a convenient approach to analyze the ^{15}N relaxation data for denatured proteins, because it requires few assumptions about the form of either the protein motion or the spectral density function itself.[29–33] Results for both protein concentrations are shown in Figure 7 to illustrate the level of experimental uncertainty and the influence of the residual association reaction.

Residues M26, Y27 and G29, which are located at the center of the main association region, show a high amplitude of slow motions (high $J_{eff}(0)$). Apparently, the slow motions result from the residual self-association reaction, since they are suppressed at lower protein concentrations. Apart from these three center residues, the influence of self-association on the backbone dynamics is not significant.

Though uncertainties in the data obscure any subtle dynamics pattern, the variation in $J(\omega)$ is clear across the sequence. The N and C-terminal residues are especially flexible, which is commonly referred to as an end effect.[32–34] However, the dynamic profile does not follow a classic bell-shaped curve of disordered linear polymers, with a flexible terminus and a restricted center region.[35] Residues 53-63 in the center of the G88W110 sequence are more flexible. The least flexible regions comprise residues 13-39 and 78-96.

These variations in mobility mainly occur on the nanosecond to picosecond timescale. The variations of $J(\omega)$ values at three frequencies generally correlate: the most restricted region 78-96 has increased $J_{eff}(0)$ values accompanied by corresponding increases in $J(\omega_N)$ and decreases in $J(\omega_H + \omega_N)$; the flexible region 53-63 has decreased $J_{eff}(0)$ values accompanied by corresponding decreases in $J(\omega_N)$ and increases in $J(\omega_H + \omega_N)$. The correlation indicates that the major variation in backbone dynamics is not caused by slow motions on the millisecond to microsecond timescale, since intermediate exchange would influence only $J_{eff}(0)$. That varying the CPMG spin echo refocussing delay in the R_2 experiments did not significantly influence the R_2 rates (data not shown) also indicates the lack of slow motion for most residues.

Discussion

Association region

In a system with multiple conformers interconverting on the fast to intermediate NMR timescale, the transverse relaxation rates and the average chemical shifts of nuclei are determined by the relative population of each conformer and their interconverting rate.[36,37] The association exchange of denatured SNase was estimated to occur on a timescale of approximately 0.1 ms,[36] since the increased R_2 of 1.5 mM G88W110 in 4 M urea could be significantly suppressed by reducing the spin echo delay δ in the CPMG pulse sequence from 1 ms to 250 μs (data not shown). The population variations of associated molecules of denatured SNase were manifested by the concentration-dependence of the line broadening and the H_N chemical shifts. They provide evidence of a self-association reaction at the residue level.

Figure 8(a) maps the two regions involved in association observed in the urea-denatured G88W110 onto its folded structure. Residues 13-39, constituting the strands β1-β2-β3 and a hydrophobic stretch in the native structure, display the most significant concentration dependence of exchange line broadening and H_N chemical shifts for G88W110 and Δ131Δ. This suggests strongly that they form the main association interface. Similar concentration-dependant line broadening was observed in the same peptide region for wild-type SNase in 4 M urea and a physiologically denatured 58-residue fragment spanning the main region involved in association (K.Y. & J.W., unpublished observations). These observations indicate that the chemical exchange of residues 13-39 in denatured states of SNase mainly originates from a self-association reaction involving this region. However, the interpretation of previous reports has considered the same observations in Δ131Δ as the result of chemical exchange due to intramolecular motion.[15,16]

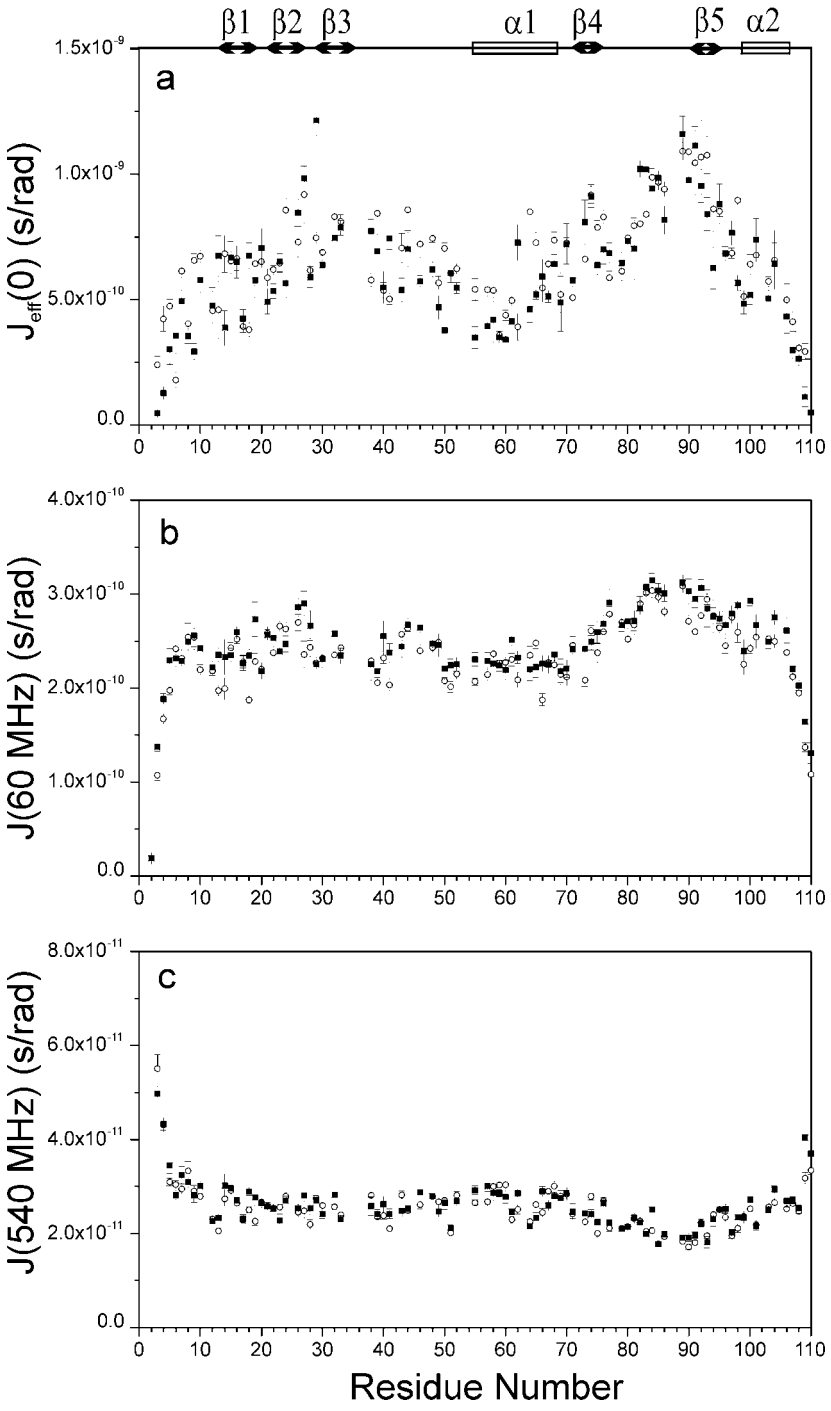

Figure 7. Spectral density function of G88W110 at (a) 0 Hz, (b) 60 MHz and (c) approximately 540 MHz deduced from the R_1 and R_2 ($\delta = 500$ μs) rates and the steady-state {^{1}H-^{15}N} NOE enhancements in 6 M urea, 305 K and protein concentrations of 1.5 mM (filled square) and 0.4 mM (open circle).

In the main region involved in association, residues located in strand β1 appear to be less stable in the associated state because in the β1 region the ''residual'' structure is more easily disrupted by urea,[15] the chemical exchange is less affected by the association reaction at low protein concentrations (Figure 4) and the H_N chemical shifts are less disturbed by the association reaction (Figure 5).

In addition to the main region involved in association, we observe a second region involved in association in urea-denatured G88W110. The precise boundary of the second association region cannot be determined due to the weakness of the effects. It may involve either a narrower range of residues 88-96 spanning a turn and strand β5 or a broader range of residues 79-105 which form a loop, strand β5 and helix α2 in the folded nuclease. The associated states are likely to be heterogeneous with respect to the second association region, which may participate in the associated state formed by the main association region, or alternatively may associate independently of the main association reaction. To define which mechanism occurs or whether both occur will require further study.

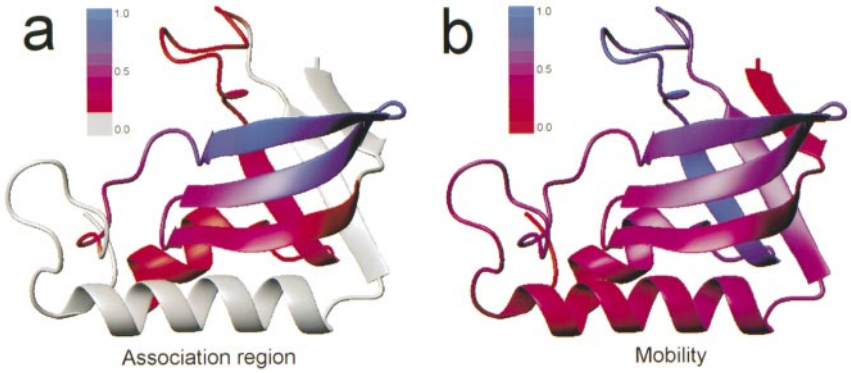

Figure 8. Schematic diagram illustrating the (a) association region and the (b) backbone flexibility in the urea-denatured G88W110 fragment of staphylococcal nuclease. (a) Association region. The involvement in the association reaction of each residue was quantified as follows. The increase of the R_2 rate shown in Figure 3(b) and the absolute H_N chemical shift movement shown in Figure 4(a) with G88W110 concentration increasing from 0.1 mM to 1.5 mM in 4 M urea were smoothed, normalized, and added to give the final association index. The color scheme is a linear mixture of blue and red, with the blue fraction proportional to the association index. The blue region is the main association region in strands β2 and β3. The red region is less involved in the association reaction, including strand β1 and the second association region centered on strand β5. In order to clearly illustrate the minor association region, the residues with association indices less than 0.2 (considered as not being involved in the association reaction) are not colored. (b) Backbone flexibility. The two $J_{eff}(0)$ values for unfolded G88W110 fragments in 6 M urea at protein concentrations of 1.5 mM and 0.4 mM were averaged, smoothed and used as a mobility restriction index. The color scheme is the same as for graph a with the blue fraction proportional to the mobility restriction index. The most restricted residues 78-96 are blue. Terminal ten residues and residues 53-63 are the most flexible and are colored red. These Figures were produced by MOLMOL.[46] The G88W110 structure is faithful to the corresponding part of the native structure of the full length nuclease (PDB entry 1stn).

We are unable to observe the second association region in Δ131Δ, most likely because of the following reasons: (1) The tryptophan substitution at residue 88 increases the hydrophobicity of this region, which may favor the association reaction in G88W110. (2) The 50 mM acetate buffer used in G88W110 samples might increase the degree of association (see below). (3) Because of the different denaturing conditions, the observed course of change of association equilibrium is not the same for Δ131Δ and G88W110. For G88W110 denatured in 4 M urea the equilibrium shifts from a weakly associated state at 1.5 mM protein to a state nearly free of association at 0.1 mM protein. While for Δ131Δ, the equilibrium shifts from a predominantly associated state at 2 mM protein to a weakly associated state at <0.1 mM protein. A state with no significant degree of association cannot be reached for Δ131Δ. It is likely that the course of change observed for G88W110 in 4 M urea is comparable to the course that would be observed for Δ131Δ if it were possible to move to even lower protein concentration ($\ll$10 μM).

Structure of the associated state

Structural information about the associated state can be inferred from the disturbance of the unfolded monomer by the association reaction. As the associated states are favored at high protein concentration, the positive changes in H_N chemical shift (Figure 5) suggest that the associated state has mainly β-sheet conformation in both the main and second association regions, including the native-like hairpin of strands β2 and β3. Previous studies based on an alternative method that followed the carbon chemical shift with increasing urea concentration have pointed out that the residual structure formed by residues 13-39 in denatured Δ131Δ is a β-meander.[15]

It is very likely that hydrophobic interactions play an important role in stabilizing the associated states, since glycine substitutions of the hydrophobic residues in region 13-39, such as V23G, F34G, L36G, L37G, L38G and V39G, greatly alleviated the line broadening in Δ131Δ.[16] Moreover, both the main and second association regions are hydrophobic stretches in the sequence of SNase.

Strongly and weakly associated states

G88W110 and Δ131Δ shown different degrees of self-association in the range of protein concentrations examined. Based on the apparent molecular size, the associated states of Δ131Δ at physiological conditions can be classified into the strongly associated state (>0.4 mM protein concentration) in which oligomeric forms dominate and the weakly associated state (<0.4 mM protein concentration) in which monomeric forms dominate. However, only weakly associated states were observed for 1.5 mM G88W110 in 4 M urea, as apparently the denaturant urea disfavors the associated state.

The molecular radius of 2 mM Δ131Δ (40 Å), which is in the strongly associated state, is nearly double that of the mostly monomeric state at concentrations below 0.4 mM (Figure 6). Depending on the molecular shape, the apparent molecular mass is proportional to the square of the radius for a random coil conformation and to the cube of the radius for a solid sphere shape.[27] Doubling the

radius requires a fourfold increase of the molecular mass for the random coil conformation and an eightfold increase of the molecular mass for the solid sphere shape. Therefore, the degree of multimerization of 2 mM Δ131Δ is estimated to be equivalent to a 4 to 8 mer. It is very likely that heterogeneous multimers of various sizes are in equilibrium in the solution.

For a structured molecule with the size of a 4 to 8 mer of Δ131Δ (MW = 60-120 kDa), the slow molecular tumbling rate would cause very broad line widths. Though the residues in the main association region of Δ131Δ are broadened beyond detection in the strongly associated state, other residues have quite narrow line widths characteristic of relatively high mobility. A model of the associated state consistent with these observations is that residues 13-39 form a native-like core structure and the remainder of the polypeptide chain remain highly disordered in the associated state. The transverse relaxation rate of the nuclei in the core structure could be increased by the slow correlation rate of the overall molecular tumbling and the monomer-oligomer and/or oligomer-oligomer chemical exchange processes. The relaxation mechanisms of the remaining residues are mainly determined by local fast motions rather than the overall slow tumbling rate, which explains why these residues still show ''normal'' behavior in the strongly associated state.

For the weakly associated states of Δ131Δ below 0.4 mM and G88W110 in 4 M urea, the apparent molecular radii change slightly as a function of protein concentration and are approximately equal to that of the 1-136 fragment of SNase in the monomeric state. This suggests that a large fraction of both Δ131Δ and G88W110 molecules are in the monomeric state under these conditions. Resonances of all residues of Δ131Δ and G88W110 are visible in the ^{1}H-^{15}N HSQC spectrum for weakly associated states, and the chemical shifts of resonances including those broadened due to association exchange are close to the random coil values, indicating that the unfolded monomer is the predominant state. The fraction of associated molecules can be estimated for 1.5 mM G88W110 in 4 M urea by chemical shift and molecular size data: H_N chemical shift deviation gives a lower limit of 1-5% associated molecules and the molecular size change predicts a 30% or 50% increase in the apparent molecular mass referred to random coil or solid sphere conformations, respectively. These estimates suggest that only a small amount of associated species is required to produce significant line broadening.

In the case of G88W110 in 4 M urea, the line broadening could be largely suppressed by reducing the protein concentration to 0.1 mM. This means that most of the chemical exchange under these conditions arises from the association reaction. However, in Δ131Δ the residues from strands β2 and β3 still have very weak intensities at 20 μM, showing that chemical exchange remains pronounced in the lowest protein concentration tested here. In principle, the residual chemical exchange may arise from monomer-oligomer exchange and/or from intramolecular motion. Several lines of evidence listed below support monomer-oligomer equilibrium being the dominant exchange mechanism for Δ131Δ at low protein concentrations, despite the small fraction of oligomer: (1) A sight decrease in degree of association is observed as the Δ131Δ concentration is decreased below 0.4 mM, as shown by the consistent increase in the relative peak intensities of residues in the main association region (Figure 4(c)) and the slow decrease in the apparent molecular size (Figure 6). (2) The association equilibrium of Δ131Δ at low protein concentrations and of 1.5 mM G88W110 in 4 M urea are comparable. The intensity ratios of G29:G55, M32:G55 and T33:G55 are 0.15, 0.19, and 0.28 for 0.1 mM Δ131Δ without urea and are 0.11, 0.20 and 0.23 for 1.5 mM G88W110 in 4 M urea, indicating similar degrees of line broadening. Since the self-association reaction is the major cause of the line broadening of the urea-denatured G88W110, it is likely that association is the same major cause for the similar broadening of Δ131Δ at low protein concentrations. (3) The absence of urea in the Δ131Δ solution probably causes the association reaction to shift to lower protein concentrations and the association equilibrium to become less sensitive to the protein concentration. The exchange line broadening for Δ131Δ may continue to decrease at lower protein concentrations ($\ll$20 μM). However, such concentrations are not accessible to current NMR techniques.

As it is not possible to obtain a state free of exchange line broadening for Δ131Δ solely by decreasing the protein concentration, other mechanisms such as local conformation conversion cannot be excluded at present.

It seems difficult to detect the small fraction of associated species when measuring the global property of the molecular size. The weak decrease of the apparent molecular size of Δ131Δ below 0.4 mM concentration may be mistakenly regarded as normal baseline variation (Figure 6). Indeed, previous small angle X-ray scattering and gel filtration examinations detected no aggregation in Δ131Δ.[12,16] Even a small amount of association can significantly affect the backbone dynamics at the residue level. This indicates that examination of the concentration dependence of the backbone dynamics is a more sensitive approach to detect weak levels of association.

Comparison with association in related proteins

Self-association of molecules under acid-denatured conditions has been observed for SNase[5,6] and two other OB-fold proteins, CspA[7] and LysN.[8] The comparison of the present investigations with these highly relevant examples is

important for understanding the principle and pattern underlying protein aggregation.

Depending on the nature and concentration of anions and also the concentration of protein, acid-denatured SNase forms aggregates with different amounts of native-like structure, which can ultimately lead to precipitates as the aggregates exceed a specific size.[5,6] The native-like structure in aggregates of SNase increases with the increasing degree of multimerization.[5,6] Native-like structure is also formed in a soluble aggregate of LysN[8] and was temporarily formed for CspA during the lag phase of polymerization, which ultimately developed into insoluble amyloid fibrils consisting mainly of β-strand.[7] Under the conditions of the present study, however, native overall structure of SNase was not observed upon association except that the local β1-β2-β3 meander was found to be native-like in the aggregates. The association reactions examined here are reversible and do not lead to insoluble aggregates during the entire course of the experiment.

The main association interface of denatured SNase under close to neutral conditions involves the β1-β2-β3 region. Interestingly, the regions that are mainly responsible for initialization of aggregation in LysN[8] and aggregation growth in CspA[7] are the same as for SNase in the topology. This suggests that there are similar association mechanisms for the above three OB-fold proteins. One possible explanation is that all three of these regions are hydrophobic.

It has been shown that anions can induce association of acid-denatured protein by screening the electrostatic repulsion between positive charged groups at low pH.[5,6,8] A similar mechanism has been proposed for anion induced folding of acid-denatured proteins into a more structured A-state.[38,39] In a preliminary study, we have observed that the association reaction of denatured SNase at pH ~ 5.0 also seems to be sensitive to the ionic strength or anion concentration. When 0.1 mM Δ131Δ is dissolved in 50 mM acetate buffer or 50 mM KCl solution, the HSQC spectra are much poorer than those obtained in aqueous solution alone, suggesting that the higher ionic strength can increase the degree of aggregation. The 50 mM acetate buffer used in urea-denatured G88W110 samples might therefore increase the degree of association. However, the conclusions of the present study still hold, since both fragment samples have nearly constant ionic strength as the protein is diluted. It should be noted that the ionic strength is not the same for the samples of Δ131Δ and G88W110. The pH of Δ131Δ samples were brought to 5.3 by small amounts of HCl without other buffer or salt solutions, following the same procedure as in the previously reported studies on Δ131Δ.[12] The ionic strength of Δ131Δ samples can thus be maintained at a minimal level of Cl^- < 10 mM for 1.5 mM protein as estimated by the quantity of HCl added to adjust the pH value. Hence, the Cl^- concentration variation caused by the sample dilution is in the range of approximately 1-10 mM, which would not significantly influence the association reaction.[8] For all G88W110 samples, except those used for diffusion coefficient measurements in ^2H_2O which contains no buffer, the ionic strength was kept constant by using 50 mM acetate buffer.

It is interesting that the association reaction observed at close to neutral conditions may be related to the anion-induced association of SNase under acidic conditions (pH 2.5).[5,6] NMR study of the acid-denatured but soluble SNase (1.5-3 mM) at pH 3.0 and low salt concentration (30-40 mM Cl^-) has shown that acid-denatured SNase and Δ131Δ under physiological conditions have similar NMR properties, with resonances from region β1-β2-β3 severely broadened in both states.[15] We have observed that the chemical exchange at this region for acid-denatured SNase is also sensitive to the protein concentration and Cl^- concentration (K.Y. & J.W., preliminary results), suggesting the occurrence of an association reaction. The initial association involving this region may develop into higher order aggregation as the anion and protein concentrations are increased.

Backbone dynamics of G88W110 in 6 M urea

Except for the terminal residues, the backbone dynamics of G88W110 in 6 M urea show a non-uniformity feature. Figure 8(b) schematically maps the mobility of denatured G88W110 onto its folded state. The flexible segment 53-63 spans a loop and the first half of helix α1, whereas the relatively restricted regions 13-39 and 78-96 mainly form β-strands in the folded state. A similar variation in backbone dynamics long the sequence has been observed for other unfolded proteins.[32–34]

Restricted mobility around residues 79-115 has been observed for Δ131Δ denatured under physiological conditions (residues 13-39 are invisible under these conditions).[13] The results presented here demonstrate that essentially the same mobility is maintained for G88W110 under the more denaturing conditions of 6 M urea, although for a narrower region, which can be ascribed to the high degree of flexibility of residues near the shorter C terminus of the G88W110 fragment. In addition residues 75-105 show exclusive positive values of steady-state $\{^1H\text{-}^{15}N\}$ NOE enhancements for G88W110 in 6 M urea (data not shown), agreeing with the findings for Δ131Δ.[13] This indicates that the restricted backbone motions on the nano- to picosecond timescale in this region arise from intrinsic properties of the amino acid sequence, and are essentially unaffected by the degree of denaturation and association.

Residual structure is often associated with restricted flexibility in denatured proteins.[32–34] Residues 83-86 and 94-97 in the most restricted region 78-96 form two β-turn structures in the folded structure of SNase. The two turns structures are the most persistent local structural elements in

Δ131Δ,[12,17] and retain the highest preference for turn-like conformation for G88W110 in 6 M urea (data not shown), suggesting a structural basis for the restricted mobility. The residual structure and restricted mobility in denatured polypeptide may play a role in the initialization of protein folding.

Conclusions

We have found that denatured staphylococcal nuclease self-associates at close to neutral pH. The main association reaction involving residues 13-39 causes the apparent residual β-sheet structure in this region. Depending on the degree of denaturation and protein concentration, the degree of association may be weak, but still leads to significant line broadening of the resonances of those residues involved in the association reaction. We consider that the weak association reaction should be carefully examined in the study of denatured proteins.

Materials and Methods

Sample preparation

The G88W110 fragment, containing residues 1-110 of staphylococcal nuclease and mutation G88W, was expressed and purified according to the procedures described, except that the size-exclusion column step was omitted.[21] The Δ131Δ gene, corresponding to residues 1-3 and 13-140, was constructed using a polymerase chain reaction, cloned into the pET-3d vector and sequenced. The Δ131Δ protein was prepared in the same way as G88W110. The purified proteins were extensively dialyzed against deionized water and against Milli-Q water in the final step before being lyophilized. Uniformly ^{15}N and $^{15}N/^{13}C$-labeled samples were obtained through bacterial growth in M9 minimal media using ^{15}N-labeled ammonium chloride (1 g/l) and ^{13}C-labeled glucose (2 g/l), when required, as the sole nitrogen and carbon sources.

NMR samples of G88W110 consisted of 1.5, 0.4 and 0.1 mM protein, 4 or 6 M urea, and 50 mM deuterated acetate buffer (pH 4.9, 10 % $.^2H_2O$). For consistency with previous experiments done by the Shortle's group,[12] the Δ131Δ was dissolved in 90 % H_2O/10 % $.^2H_2O$ with no added buffer or salt, and brought to pH 5.3 by the addition of HCl. The protein concentration was calculated by the mass of the protein powder. The samples of different protein concentrations were prepared from the same stock solution.

NMR spectroscopy

All multidimensional NMR experiments were carried out on a Bruker DMX 600 spectrometer equipped with an inverse triple-resonance three-axis gradient probe. All measurements were made at 305 K. Three-dimensional experiments of HNCO, HN(CA)CO, CBCA(CO)NH, HNCACB,[40] H(CCO)NH[41] with a ^{13}C isotropic mixing time of 16 ms and ^{15}N-TOCSY-HSQC with an isotropic mixing time of 60 ms were recorded on a 2.5 mM ^{15}N, ^{13}C-labeled G88W110 in 6 M urea. The references for most of the experiments related to here can be found in reference 37. Most of these experiments incorporated echo-antiecho gradient selection and sensitivity enhancement.[42]

All data were processed and analyzed using Felix 98 (Biosym/MSI). The data points in each indirect dimension were usually doubled by linear prediction[43] before zero filling to the appropriate size. A 90 to 60° shifted square sine bell apodization was used for all three dimensions prior to Fourier transformation. ^1H chemical shifts were referenced to internal 2,2-dimethyl-2-silapentane-5-sulfonate (DSS). ^{15}N and ^{13}C chemical shifts were referenced indirectly.[37]

^{15}N R_1 and R_2 relaxation rates, and steady-state {^1H-^{15}N} NOE enhancements were determined for urea-denatured G88W110 by standard methods.[44] R_1 relaxation delays were set to 10, 60, 120, 240, 360, 530, 760 and 1150 ms. R_2 relaxation delays were set to 8, 24, 40, 64, 88, 112, 144 and 192 ms. R_2 experiments were recorded with CPMG spin echo delays of 1 ms, 500 μs and 250 μs. The recycle delay for the R_1 and R_2 experiments was 1.1 seconds. The acquisition dimension contained 1024 complex points and was zero filled twofold. The ^{15}N dimension contained 128 complex data points which were extended to 228 points by linear predication and then zero filled to 512 points. Peak intensities were fitted to a two-parameter monoexponential decay function to determine R_1 and R_2 rates for individual amide protons. Rates and uncertainties were estimated using the Levenberg-Marquardt algorithm in the program gnuplot (ftp://ftp.dartmouth.edu/pub/gnuplot). In the NOE experiment, a delay of 2 seconds was followed by ^1H saturation for 3 seconds. In the control experiment the saturation period was replaced by a delay of equivalent duration (3 seconds). The total recycling delay for both experiments was thus 5 seconds. NOE and control experiments were interleaved. The steady-state {^1H-^{15}N} NOE enhancements were calculated as the ratio of peak heights from spectra obtained with and without presaturation of amide proton resonances. Errors were estimated from the root-mean-square noise of the spectra.

Diffusion coefficient measurement

The diffusion coefficient D was measured by pulse-field gradient spin echo NMR by using the PG-SLED sequence.[25,26] For unrestricted diffusion of a molecule in an isotropic medium, the observed signal intensity (I), relative to the signal in the absence of PFGs (I_0), is given by:[24]

$$I - I_0 \exp(-(\gamma\delta G)^2(\Delta - \delta/3)D) \qquad (2)$$

where G and δ are the magnitude and duration of the field-gradient pulses, respectively, Δ is the time between field-gradient pulses, and γ is the magnetogyric ratio of hydrogen. A series of 15 spectra were obtained, with the delay periods ($\delta = 6$ ms, $\Delta = 50$ ms) held constant and the gradient strength incremented in steps from 2 to 56 % of the calibrated maximum strength of our probe (70 G/cm). Δ131Δ with concentrations of 10 μM to 2 mM was dissolved in ^2H_2O, p^{2}H 5.3. G88W110 with concentrations of 1.5 mM, 0.4 mM and 0.1 mM was dissolved in ^2H_2O, with 4 M deuterated urea, p^{2}H 4.9. No buffer is employed to avoid introducing extra proton resonances in the 1D ^1H spectrum. Dioxane at a concentration five times the protein concentration was added as a radius standard allowing possible changes in the solution viscosity to be monitored.[26] The protein diffusion coefficient was obtained by integrating the methyl region

(1.0-0.7 ppm), and fitting the resulting intensities to equation (2). The low signal-to-noise ratio for samples at low protein concentrations was overcome by using the most intense methyl region in the analysis. *D* values obtained from other regions were the same within the experimental uncertainties. Because the dioxane signal resonates at a frequency where signals arising from the protein also resonate, its integrated signal was fit to a sum of two decaying Gaussians terms, one of which was constrained to have the same decay rate as that observed for the protein.[26] The data were fit using the program gnuplot.

Reduced spectral density mapping

The frequency spectrum for the random rotational motion of the ^{15}N-^{1}H bond vector was described by the spectral density function $J(\omega)$. Assuming that the $J(\omega)$ values are the same at the frequencies $\omega_H - \omega_N$, ω_H and $\omega_H + \omega_N$, the $J(\omega)$ values at 0, ω_N, and $\omega_H + \omega_N$ can be extracted from the ^{15}N R_1 and R_2 relaxation rates and the steady-state $\{^{1}H$-$^{15}N\}$ NOE enhancements by reduced spectral density mapping.[29–31] Because the $J(0)$ value may contain a contribution from chemical exchange (R_{2ex}), a more general term $J_{eff}(0)$ is used here. In fact, the chemical exchange is negligible for most residues of G88W110 in 6 M urea. Uncertainties in the values of the spectral density function were determined using a Monte Carlo procedure based on the uncertainties in the measured relaxation parameters.[32]

Acknowledgments

We thank Professor John L. Markley and Frits Abildgaard (University of Wisconsin-Madison) for providing the pulse programs, Sarah Perrett for critically reading the manuscript. This research was supported by Grants No. 39570170 and 39823001 from the China Natural Science Foundation.

References

1. Fink, A. L. (1998). Protein aggregation: folding aggregates, inclusion bodies and amyloid. *Fold. Design*, **3**, R9-R15.
2. Rochet, J.-C. & Lansbury, P. T., Jr (2000). Amyloid fibrillogenesis: themes and variations. *Curr. Opin. Struct. Biol.* **10**, 60-68.
3. Speed, M. A., King, J. & Wang., D. I. C. (1997). Polymerization mechanism of polypeptide chain aggregation. *Biotechnol. Bioeng.* **54**, 33-343.
4. London, J., Skrzynia, C. & Goldberg, M. E. (1974). Aggregation at critical urea concentration. *Eur. J. Biochem.* **47**, 409-415.
5. Uversky, V. N., Segel, D. J., Doniach, S. & Fink, A. L. (1998). Association induced folding of globular proteins. *Proc. Natl Acad. Sci. USA*, **95**, 5480-5483.
6. Uversky, V. N., Karnoup, A. S., Khurana, R., Segel, D. J., Doniach, S. & Fink, A. L. (1999). Association of partially-folded intermediate of staphylococcal nuclease induces structure and stability. *Protein Sci.* **8**, 161-173.
7. Alexandrescu, A. T. & Rathgeb-Szabo, K. (1999). An NMR investigation of solution aggregation reactions preceding the misassembly of acid-denatured cold shock protein A into fibrils. *J. Mol. Biol.* **291**, 1191-1206.
8. Alexandrescu, A. T., Lamour, F. P. & Jaravine, V. A. (2000). NMR evidence for progress stabilization of native-like structure upon aggregation of acid-denatured LysN. *J. Mol. Biol.* **295**, 239-255.
9. Silow, M. & Oliveberg, M. (1997). Transient aggregates in protein folding are easily mistaken for folding intermediates. *Proc. Natl Acad. Sci. USA*, **94**, 6084-6086.
10. Hynes, T. R. & Fox, R. O. (1991). The crystal structure of staphylococcal nuclease refined at 1.7 angstroms resolution. *Proteins: Struct. Funct. Genet.* **10**, 92-105.
11. Murzin, A. G. (1993). OB(oligonucleotide/oligosaccharide binding)-fold: common structural and functional solution for non-homologous sequences. *EMBO J.* **12**, 861-867.
12. Alexandrescu, A. T., Abeygunawardana, C. & Shortle, D. (1994). Structure and dynamics of a denatured 131-residue fragment of staphylococcal nuclease: a heteronuclear NMR study. *Biochemistry*, **33**, 1063-1072.
13. Alexandrescu, A. T. & Shortle, D. (1994). Backbone dynamics of a highly disordered 131-residue fragment of staphylococcal nuclease. *J. Mol. Biol.* **242**, 527-546.
14. Wang, Y., Alexandrescu, A. T. & Shortle, D. (1995). Initial studies of the equilibrium folding pathway of staphylococcal nuclease. *Phil. Trans. Roy. Soc. Lond. B.* **348**, 27-34.
15. Wang, Y. & Shortle, D. (1995). The equilibrium folding pathway of staphylococcal nuclease: Identification of the most stable chain-chain interactions by NMR and CD spectroscopy. *Biochemistry*, **34**, 15895-15905.
16. Wang, Y. & Shortle, D. (1996). A dynamic bundle of four adjacent hydrophobic segments in the denatured state of staphylococcal nuclease. *Protein Sci.* **5**, 1898-1906.
17. Zhang, O., Kay, L. E., Shortle, D. & Forman-Kay, J. D. (1997). Comprehensive NOE characterization of a partially folded large fragment of staphylococcal nuclease, Δ131Δ, using NMR methods with improved resolution. *J. Mol. Biol.* **272**, 9-20.
18. Gillespie, J. R. & Shortle, D. (1997a). Characterization of long-range structure in the denatured state of staphylococcal nuclease. I. Paramagnetic relaxation enhancement by nitroxide spin labels. *J. Mol. Biol.* **268**, 158-169.
19. Gillespie, J. R. & Shortle, D. (1997b). Characterization of long-range structure in the denatured state of staphylococcal nuclease. II. Distance restraints from paramagnetic relaxation and calculation of an ensemble of structures. *J. Mol. Biol.* **268**, 170-184.
20. Sinclair, J. F. & Shortle, D. (1999). Analysis of long-range interactions in a model denatured state of staphylococcal nuclease based on correlated changes in backbone dynamics. *Protein Sci.* **8**, 991-1000.
21. Ye, K., Jing, G. & Wang, J. (2000). Interactions between subdomains in the partially folded state of staphylococcal nuclease. *Biochim. Biophys. Acta*, **1479**, 123-134.
22. Shortle, D. (1996). Structural-analysis of nonnative states of proteins by NMR methods. *Curr. Opin. Struct. Biol.* **6**, 24-30.
23. Yao, J., Dyson, H. J. & Wright, P. E. (1997). Chemical shift dispersion and secondary structure

prediction in unfolded and partly folded proteins. *FEBS Letters,* **419**, 285-289.
24. Stejskal, E. O. & Tanner, J. E. (1965). Spin diffusion measurements: spin echoes in the presence of a time-dependent filled gradient. *J. Chem. Phys.* **42**, 288-292.
25. Gibbs, S. J. & Johnson, C. S., Jr. (1991). A PEG NMR experiment for accurate diffusion and flow studies in the presence of eddy currents. *J. Magn. Reson.* **93**, 395-402.
26. Jones, J. A., Wilkins, D. K., Smith, L. J. & Dobson, C. M. (1997). Characterisation of protein unfolding by NMR diffusion measurements. *J. Biomol. NMR,* **10**, 199-203.
27. Ilyina, E., Roongta, V., Pan, H., Woodward, C. & Mayo, K. H. (1997). A pulsed field gradient NMR study of bovine pancreatic trypsin inhibitor self-association. *Biochemistry,* **36**, 3383-3388.
28. Flanagan, J. M., Kataoka, M., Fujisawa, T. & Engelman, D. M. (1993). Mutations can cause large changes in the conformation of a denatured protein. *Biochemistry,* **32**, 10359-10370.
29. Ishima, R. & Nagayama, K. (1995). Protein backbone dynamics revealed by quasi spectral density function analysis of amide N-15 nuclei. *Biochemistry,* **34**, 3162-3171.
30. Peng, J. W. & Wagner, G. (1992a). Mapping of spectral density-functions using heteronuclear NMR relaxation measurements. *J. Magn. Reson.* **98**, 308-332.
31. Peng, J. W. & Wagner, G. (1992b). Mapping of the spectral densities of N-H bond motions in Eglin-c using heteronuclear relaxation experiments. *Biochemistry,* **31**, 8571-8586.
32. Fong, S., Bycroft, M., Clarke, J. & Freund, S. M. V. (1998). Characterization of the urea-denatured states of an immunoglobulin superfamily domain by heteronuclear NMR. *J. Mol. Biol.* **278**, 417-429.
33. Meekhof, A. E. & Freund, S. M. V. (1999). Probing residual structure and backbone dynamics on the milli- to picosecond timescale in a urea-denatured fibronectin type III domain. *J. Mol. Biol.* **286**, 579-592.
34. Eliezer, D., Yao, J., Dyson, H. J. & Wright, P. E. (1998). Structural and dynamic characterization of partially folded states of apomyoglobin and implications for protein folding. *Nature Struct. Biol.* **5**, 148-155.
35. Hu, Y., Macinnis, J. M., Cherayil, B. J., Fleming, G. R., Freed, K. F. & Perico, A. (1990). Polypeptide dynamics: experimental tests of an optimized Rouse-Zimm type model. *J. Chem. Phys.* **93**, 822-836.
36. Orekhov, V., Yu., Pervushin, K. V. & Arseniev, A. S. (1994). Backbone dynamics of (1-71) bacterioopsin studied by two-dimensional ^{1}H-^{15}N NMR spectroscopy. *Eur. J. Biochem.* **219**, 887-896.
37. Cavanagh, J., Fairbrother, W. J., Palmer, A. G. & Skelton, N. J. (1996). *Protein NMR Spectroscopy*, Academic Press, San Diego.
38. Goto, Y., Calciano, L. J. & Fink, A. L. (1990a). Acid-induced folding of proteins. *Proc. Natl Acad. Sci. USA,* **87**, 573-577.
39. Goto, Y., Takahashi, N. & Fink, A. L. (1990b). Mechanism of acid-induced folding of proteins. *Biochemistry,* **29**, 3480-3488.
40. Wittekind, M. & Mueller, L. (1993). HNCACB, a high-sensitivity 3D NMR experiment to correlate amide-proton and nitrogen resonances with the alpha- and beta-carbon resonances in proteins. *J. Magn. Reson.* **101**, 201-205.
41. Grzesiek, S., Anglister, J. & Bax, A. (1993). Correlation of backbone amide and aliphatic side-chain resonances in $^{13}C/^{15}N$-enriched proteins by isotropic mixing of ^{13}C Magnetization. *J. Magn. Reson. B,* **101**, 114-119.
42. Kay, L. E., Keifer, P. & Saarinen, T. (1992). Pure absorption gradient enhanced heteronuclear single quantum correlation spectroscopy with improved sensitivity. *J. Am. Chem. Soc.* **114**, 10663-10665.
43. Zhu, G. & Bax, A. (1992). Improved linear prediction of damped NMR signals using modified forward backward linear prediction. *J. Magn. Reson.* **100**, 202-207.
44. Farrow, N. A., Munhandiram, R., Singer, A. U., Pascal, S. M., Kay, C. M., Gish, G., Shoelson, S. E., Pawson, T., Forman-Kay, J. D. & Kay, L. E. (1994). Backbone dynamics of a free and a phosphopeptide-complexed Src homology 2 domain studied by ^{15}N NMR relaxation. *Biochemistry,* **33**, 5984-6003.
45. Kraulis, P. (1991). Molscript: a program to produce both detailed and schematic plots of protein structures. *J. Appl. Crystallog.* **24**, 946-950.
46. Koradi, R., Billeter, M. & Wüthrich, K. (1996). MOLMOL: a program for display and analysis of macromolecular structures. *J. Mol. Graph.* **14**, 51-55.

Edited by P. E. Wright

(Received 5 September 2000; received in revised form 13 December 2000; accepted 12 January 2001)

http://www.academicpress.com/jmb

Supplementary Material comprising one Table is available on IDEAL